

23 **Abstract**

24 The Hans-Ertel Centre for Weather Research is a network of German
25 universities, research institutes and the German Weather Service (Deutscher
26 Wetterdienst, DWD). It has been established to trigger and intensify basic
27 research and education on weather forecasting and climate monitoring. The
28 performed research ranges from nowcasting and short-term weather forecasting
29 to convective-scale data assimilation, the development of parameterizations for
30 numerical weather prediction models, climate monitoring and the communication
31 and use of forecast information.

32 Scientific findings from the network contribute to better understanding of the
33 life-cycle of shallow and deep convection, representation of uncertainty in
34 ensemble systems, effects of unresolved variability, regional climate variability,
35 perception of forecasts and vulnerability of society. Concrete developments
36 within the research network include dual observation-microphysics composites,
37 satellite forward operators, tools to estimate observation impact, cloud and
38 precipitation system tracking algorithms, large-eddy-simulations, a regional
39 reanalysis and a probabilistic forecast test product.

40 Within three years, the network has triggered a number of activities that
41 include the training and education of young scientists besides the centre's core
42 objective of complementing DWD's internal research with relevant basic research
43 at universities and research institutes. The long term goal is to develop a self-
44 sustaining research network that continues the close collaboration with DWD and
45 the national and international research community.

46 47 **1 Introduction**

48 The increasing vulnerability of society to weather and natural disasters
49 emphasizes the need for improved forecasts and warnings (IPCC, 2012). In
50 addition, weather forecasts become increasingly important for economic
51 applications, e.g. for predicting renewable energy production and energy
52 demand. Climate change and its impact on local weather pose further risks to
53 society and economy. The Hans-Ertel Centre for Weather Research (German:
54 Hans-Ertel Zentrum für Wetterforschung¹, abbreviated as HErZ) initiated by
55 Deutscher Wetterdienst (DWD) and its scientific advisory committee intends to
56 trigger and intensify basic research in Germany that will, over the next decade,
57 lead to an improved ability to predict weather- and climate-related risks and to
58 improved warnings and communication of these predictions. In a round-table
59 discussion in 2007 that included most major German meteorological research
60 institutions, five key research areas for the further advancement of modelling,
61 monitoring and forecasting systems were identified:

- 62 • Atmospheric dynamics and predictability;
- 63 • Data Assimilation;
- 64 • Model development;
- 65 • Climate monitoring and diagnostics;

¹ <http://www.dwd.de/ertel-zentrum>

- 66 • Optimal use of information from weather forecasting and climate monitoring
67 for society.

68 In the first out of three four-year phases, these topics are addressed by five
69 branches of HErZ (table 1), which together form a virtual centre for weather and
70 climate research. This article presents the research objectives and scientific
71 highlights of the current implementation of HErZ after the first three years since
72 the centre was established in the beginning of 2011.

73 Research in the five scientific areas of HErZ has a long history. More than 100
74 years after Vilhelm Bjerknes first proposed the idea of a mathematical model of
75 the atmosphere's dynamics (BJERKNES, 1904; GRAMELSBERGER, 2009) and
76 after more than 60 years of numerical weather prediction (NWP), our ability to
77 model the atmosphere has improved drastically (BENGTSSON, 2001;
78 EDWARDS, 2010). However, fundamental advancement in our modelling
79 capabilities requires time-scales of decades and therefore long-term and
80 coordinated funding strategies. Significant shortcomings still exist, particularly in
81 our ability to accurately predict specific regional weather events (e.g. severe
82 convective systems) and the regional impact of climate change. Recent major
83 German research activities addressed the first of these topics, particularly
84 precipitation forecasts, predictability and atmospheric dynamics. These activities
85 include the Priority Program Quantitative Precipitation Forecast (HENSE and
86 WULFMEYER, 2008), the field campaign Convective and Orographically Induced
87 Precipitation Study (COPS, WULFMEYER et al., 2008) and the research group
88 PANDOWAE² (Predictability ANd Dynamics Of Weather Systems in the Atlantic-
89 European Sector). HErZ builds upon expertise gained in these recent activities,
90 but has a broader focus that inter alia also includes climate research and
91 forecasts communication.

92 Overall, the development of NWP systems is challenging for many reasons:
93 The complexity to combine observations with a model state for creating initial
94 conditions, the requirement to include all relevant processes and phenomena,
95 poor knowledge on several of these processes and technical limitations that
96 prohibit the explicit representation of processes. Development of NWP systems
97 may therefore be best achieved in a collaborative effort between the academic
98 community and operational centres (JAKOB, 2010). In the United Kingdom, the
99 Joint Centre for Mesoscale Meteorology which consists of staff from the
100 University of Reading and the Met Office exhibits an example of the fruitful
101 collaboration between academia and a weather service. HErZ addresses this
102 need in Germany and aims at closing the gap between the academic community
103 and DWD. It strengthens collaboration between universities, research institutes
104 and DWD and complements more applied internal research at DWD with basic
105 research at university and non-university institutions.

106 The intended combination of basic research with user oriented foci in weather
107 and climate research will be demonstrated by a broad selection of research
108 examples obtained during the initial phase of HErZ. Section 2 explains the
109 implementation of HErZ as a virtual centre and section 3 presents the objectives

² <http://www.pandowae.de>

110 of the current five branches of HErZ together with highlights of their scientific
111 findings. A summary and outlook follows in section 4.

112

113 **2 Implementation of the virtual centre**

114 HErZ currently consists of five branches which each have a size of about 5-6
115 positions (full-time equivalent) including two branch leaders, one from the host
116 institution and one from DWD. Most branches complemented the funding
117 provided by HErZ through the acquisition of other related research projects. The
118 branches are located at one or multiple host institutions (table 1). Regular
119 workshops and joint events ensure the interaction of different branches.

120 A key feature of HErZ is the close interaction between a national weather
121 service and basic research at universities and research institutes. This makes the
122 access to DWD facilities, data, products and end users much easier than in other
123 projects and shall ensure that the findings and developments of HErZ feed into
124 the operational modelling and forecasting chain of DWD in the longer term.

125 A further special feature for a research project is HErZ's dedication to the
126 education and training of young scientists. One component is special training
127 courses (summer or winter schools) that are also open to non-HErZ scientists.
128 Past training courses covered large-eddy-simulations, data assimilation, remote
129 sensing and forecast verification. In addition, all branches established special
130 university courses on weather and climate-related topics that were previously
131 underrepresented in the university curriculum. The integration of undergraduate
132 and graduate students is also an important educational component.

133 German research is funded by two approaches, programmatic funding for
134 applied research leading to specific developments (e.g. the base funding of DWD
135 or research institutes) and funding for basic research in any research area (e.g.
136 provided by the German Science Foundation DFG, see Volkert and Achermann
137 (2012)). HErZ exhibits an intermediate approach for basic research that is geared
138 towards long-term improvements of DWD systems.

139

140 **3 The branches of HErZ: Goals and highlights**

141 This section describes the research objectives of the current five branches of
142 HErZ and provides highlights of their scientific results from phase 1. Each branch
143 targets a different aspect of weather or climate research, but the branches share
144 common foci as for example regional high-resolution (km-scale) modelling, the
145 model representation of clouds and convection or probabilistic forecasting
146 approaches.

147

148 **3.1 Atmospheric Dynamics and Predictability**

149 HErZ-OASE (Object-based Analysis and SEamless prediction) approaches
150 seamless prediction of convective events from nowcasting to short-range
151 forecasting by merging observation-based projections and NWP. The approach
152 resides on and exploits a multi-sensor-based dual observations/microphysics 4D-
153 composite based on ground and satellite-based active and passive sensors. An
154 object-based approach to the composite allows for monitoring, characterization

155 and an improved understanding of the dynamics and life cycles of convective
156 events. Objects are identified and tracked in time by a multivariate 3D scale
157 space algorithm. The resulting data provides the core information for
158 observation-based nowcasting and NWP model initialisation and allows for its
159 merging. A climatological exploitation of the data set shall elucidate the dynamics
160 of convective events and lead to improved knowledge on predictability limits
161 including their dependence on atmospheric conditions.

162

163 **3.1.1 Synergistic use of multi-sensor data and its application**

164 The national 3D composite area currently contains weather radar,
165 geostationary satellite, and lightning detection network observations a common
166 grid at a 5 min temporal resolution. Perfect model experiments are used to
167 quantify the accuracy of radar and satellite products as well as their information
168 content for nowcasting and data assimilation (SENF et al., 2012). The current 2D
169 version contains the RADOLAN RX data from DWD's weather radar network,
170 METEOSAT SEVIRI observations and cloud products, as well as lightning
171 frequencies from the LINET network (BETZ et al., 2009). A merging scheme
172 projects dual radar observations onto a 3D polar-stereographic grid,
173 compensates for observational errors (e.g. attenuation) and mitigates advection
174 displacements caused by the 5-min volume scan intervals. The 3D high-
175 resolution composite over the Bonn-Jülich area contains besides horizontal and
176 vertical radar reflectivity Z_H and Z_V , the differential reflectivity Z_{DR} , specific
177 differential phase K_{DP} , co-polar correlation coefficient ρ_{HV} , quality indicators,
178 minimum detectable Z_H threshold and surface rain rate (RYZHKOV et al., 2013).
179 Physical downscaling is applied to enhance SEVIRI's standard $3 \times 3 \text{ km}^2$
180 resolution to $1 \times 1 \text{ km}^2$ (DENEKE and ROEBELING, 2010; BLEY and DENEKE,
181 2013). A multivariate 3D scale-space tracking algorithm based on the mean-shift
182 method (COMANICIU and MEER, 2002) is applied to the composite and will
183 evolve into a novel nowcasting framework. Its nowcasting skill is expected to
184 outperform approaches residing on single data sources (WAPLER et al., 2012)
185 and to increase the nowcasting horizon (SIEWERT et al., 2010; DIETZSCH,
186 2012). The data set allows also for a detailed regime-dependent analysis of the
187 spatial and temporal occurrence of thunderstorms (WAPLER, 2013; WAPLER
188 and JAMES, 2014) and reveals conditions and highlights regions favourable for
189 thunderstorm development.

190

191 **3.1.2 Object-based approach to weather analysis**

192 Seam-less prediction is approached by the inclusion of process information in
193 nowcasting and by assimilation of a highly-resolved radar data (MILAN et al,
194 2014). The Local Ensemble Transform Kalman Filter (LETKF; HUNT et al., 2007)
195 within the experimental KENDA (KM-scale ENsemble-based Data Assimilation;
196 REICH et al., 2011) system for the COSMO (Consortium for Small-scale
197 MOdeling) model is applied to investigate the impact of radar observations on the
198 representation of convective systems.

199 Current nowcasting strategies mostly follow advection-based strategies. Their
200 major limitation is the disregard of life-cycle effects and the inability to consider

201 emerging cells. Within HERZ-OASE an object-based analysis condenses the
202 time-space distribution of observables and related microphysics into process-
203 oriented descriptors, which may serve as proxies of the precipitation process and
204 describe macrophysical structures and microphysical processes as the trend in
205 brightband intensity or the efficiency of the raining system (e.g. TRÖMEL et al.,
206 2009; Rosenfeld et al., 1990). These can be easily exploited in nowcasting
207 methods. E.g. a reversal of the cloud-droplet effective radius (R_{eff}) tendency
208 concurrent with increasing cloud optical thickness (COT) and liquid / ice water
209 path (LWP, IWP) precedes thunderstorm intensification and lightning activity
210 (HORVÁTH et al., 2012). KONRAD-derived (*KONvektionsentwicklung in*
211 *RADarprodukten*, convection evolution in radar products) cell tracks during
212 summer 2011 show a strong correlation between COT, LWP, IWP and total
213 lightning during both the growing and the decaying phase of R_{eff} . Thus thicker,
214 wetter clouds produce more lightning (Fig. 1a, c and d). The relationship between
215 R_{eff} and total lightning, however, is more complex. Total lightning shows a strong
216 increase after the trend reversal in R_{eff} (Fig. 1b and d). Some theories postulate
217 an increase in lightning activity when large ice particles aloft precipitate in the
218 lower mixed-phase cloud region, which is consistent with the observed negative
219 correlation between flash count and cloud-top R_{eff} and the observed mean time
220 difference between the peaks in lightning and R_{eff} . For stronger storms, peak
221 lightning activity increasingly lags peak R_{eff} by up to 25-30 min for the most
222 intense storms. The observed lags presumably correspond to the time required
223 for large cloud-top ice particles to fall and intensify charge separation. Analyses
224 of convective cells captured with the polarimetric X-band radar in Bonn (BoXPo)
225 after the R_{eff} -maximum confirm the occurrence of graupel and support the
226 hypothesis that the trend reversal in R_{eff} indicates the onset of the charge
227 separation. Graupel is associated with high reflectivities Z_H and diminishing
228 differential reflectivity Z_{DR} (Fig.2). The hydrometeor classification scheme (ZRNIC
229 et al., 2001) confirms the presence of graupel in the mid and lower cloud region
230 and smaller ice particles aloft. In agreement with the 3-body scattering signature
231 visible in Fig. 2, a region with large hail particles has been identified. The
232 signature appears as a radially oriented spike of weak Z_H protruding from the far
233 side (relative to the radar) of the storm and a band of extremely large Z_{DR} values.
234 The comparison of object evolutions in observations and models can be
235 applied for model evaluation, because deviations may hint at processes not
236 adequately simulated (e.g. TRÖMEL and SIMMER, 2012). Polarimetry is
237 expected to be particularly beneficial for the evaluation of microphysical
238 processes. A prominent example is the backscatter differential phase δ , which is
239 an indicator for the dominant size of rain drops or wet snowflakes. Its
240 consideration allows for a better characterization of the brightband and can be
241 utilized for improving microphysical models (TRÖMEL et al., 2013a, 2013b).
242 Another example is the derivation of synthetic cloud products from model
243 forecasts. The frequency and size of convective cells derived by the NWC SAF
244 Rapidly Developing Thunderstorm product for observations and COSMO
245 forecasts can be used as metric for the model's ability to simulate appropriate cell
246 types (REMPEL, 2013).

247

248 **3.2 Data Assimilation**

249 Compared to global scales, research for convective-scale (km-resolution) data
250 assimilation is at a much less mature stage and it remains to be answered which
251 methods can cope with the strong non-linearities typically encountered on this
252 scale while meeting the demands for computational efficiency and frequent
253 analysis updates. Ensemble methods are seen as a promising approach to
254 address the limited predictability of small-scale systems (e.g. convection), but
255 knowledge is particularly missing on the appropriate representation of model
256 error, the choice of specific observations for these scales and the best way to
257 assimilate them. Satellite instruments nowadays provide a vast amount of
258 information on the atmospheric state, but only a very small fraction is used in
259 current convective-scale assimilation systems. Based on these shortcomings,
260 HErZ Data Assimilation (HErZ-DA) addresses four research topics: Data
261 assimilation methodology for strongly non-linear dynamics, the online estimation
262 of the impact of different observations, the representation of uncertainty in
263 ensemble systems and the improved use of cloud-related satellite observations.
264 The satellite part comprises efforts to assimilate visible (VIS) and near-infrared
265 (NIR) satellite reflectance and the development of a height correction for cloud
266 motion vectors based on satellite lidar observations.

267

268 **3.2.1 Data assimilation methodology**

269 Limited computational resources prohibit testing multiple data assimilation
270 methods extensively in a full NWP system and traditional test models for global-
271 scale data assimilation (e.g. LORENZ, 1995) are missing key features of
272 predominant convective-scale processes. To address this, a hierarchy of
273 idealized models that resemble convective-scale dynamics has been developed.
274 This hierarchy is used to test data assimilation algorithms that were generally not
275 designed for the non-linearity and non-Gaussian error structures encountered on
276 these scales. At the lowest level of complexity, CRAIG and WÜRSCH (2013)
277 introduced a simple stochastic 1D cloud model based on a spatial Poisson birth-
278 death process. At the second level, WÜRSCH and CRAIG (2014) modified the
279 shallow-water equations to introduce convection. This model represents
280 conditional instability whenever the water level exceeds a certain threshold and
281 includes the negative buoyancy effect of rainwater that limits the growth of
282 convective clouds. For both models, three data assimilation algorithms, the
283 LETKF, Sequential Importance Resampling (SIR; VAN LEEUWEN, 2009) and
284 the Efficient Particle Filter (VAN LEEUWEN, 2011) are being tested.

285 At the third level, idealized perfect model experiments are performed using the
286 experimental KENDA-COSMO system with 2 km grid spacing. These studies
287 focus on radar assimilation and the preservation of physical properties following
288 JANJIC et al. (2014). A model run with idealized initial conditions is taken as
289 “truth” (referred to as nature run) and observations simulated from this nature run
290 are used to investigate different settings or implementations of KENDA.

291 LANGE and CRAIG (2014) tested the assimilation of radar reflectivity and
292 Doppler velocity in KENDA using a nature run initialized with one vertical

293 sounding and small random perturbations to trigger convection. The major focus
294 was the comparison of the following two setups: One producing initial conditions
295 with high-resolution fine assimilation (FA) settings every 5 min and the other
296 producing initial conditions with spatially coarse assimilation (CA) settings every
297 20 min. The fine assimilation converged closely to the observations whereas the
298 coarse analysis was not able to resolve all storm details (compare Figs. 3a, b
299 and c). However, due to the limited predictability of convective-scale dynamics
300 and imbalances in the strongly forced fine assimilation, the forecasts initialized
301 from fine initial conditions quickly lost their superiority and the errors of vertical
302 velocity were similar for both experiments after 1-2 h lead time (Fig. 3d).

303

304 **3.2.2 Observation impact**

305 Knowledge about the contribution of different observations to the reduction of
306 forecast errors (referred to as observation impact) is crucial for both the
307 refinement of observing as well as data assimilation systems. However, the direct
308 calculation through numerical data denial experiments (i.e. parallel experiments)
309 is only feasible for specific applications and data sets due to computational
310 expenses. Therefore, a computationally inexpensive ensemble-based method for
311 estimating observation impact following KALNAY et al. (2012) has been
312 implemented in KENDA-COSMO (SOMMER and WEISSMANN, 2014).

313 Figs. 4a and b exemplarily illustrate the (positive and negative, respectively)
314 impact values of all observations in one particular assimilation cycle. Consistent
315 with previous studies using adjoint estimation methods (e.g. WEISSMANN et al.,
316 2012), only slightly over 50% of the observations (on average 54%) contribute to
317 an improved forecast due to the statistical nature of observation impact.

318 The ensemble impact estimation has been systematically tested by
319 comparison to data denial experiments that exclude particular observation types
320 (SOMMER and WEISSMANN, 2014). Fig. 4c shows the estimated radiosondes
321 impact and their impact in data denial experiments. Overall, the method is able to
322 reproduce the general behaviour of the impact despite deviations for individual
323 analysis cycles. Averaged over all observations during nine analysis cycles, the
324 relative deviation between the estimated and the data denial impact is about 10%
325 for different observation types. In addition, the differences were shown to be
326 statistically not significant.

327

328 **3.2.3 Representation of uncertainty**

329 This part of HErZ-DA intends to improve the representation of uncertainty in
330 ensemble systems. A first study examined the relative contribution of different
331 perturbations in the current regional COSMO ensemble prediction system of
332 DWD (KÜHNLEIN et al., 2014). The impact of initial condition perturbations that
333 are downscaled from a global multi-model ensemble was largest in the first six
334 forecast hours. Thereafter, lateral boundary condition and physical parameter
335 perturbations become more important. The impact of parameter perturbations is
336 particularly important during weak large-scale forcing of precipitation (KEIL et al.,
337 2014). Ensemble assimilation systems as KENDA directly provide an estimate of
338 initial condition uncertainty. Ongoing studies investigate the structure and growth

339 of KENDA perturbations and test different methods to account for model errors,
340 e.g. relaxation to prior spread and a stochastic boundary layer scheme.

341

342 **3.2.4 Satellite cloud observations**

343 Traditionally, VIS and NIR satellite channels have been neglected for data
344 assimilation due to the lack of suitable fast observation. Given that convective
345 systems are much earlier discernible through their cloud signal than through
346 radar observations of precipitation, these cloud-related observations are seen to
347 be particularly valuable for convective-scale modelling. HErZ-DA has developed
348 a suitable operator for assimilating VIS and NIR satellite reflectance in KENDA
349 (KOSTKA et al., 2014) and the assessment of their impact in KENDA is ongoing.
350 In addition, research in HErZ-DA uses CALIPSO (Cloud-Aerosol Lidar and
351 Infrared Pathfinder Satellite Observations) information to correct the height
352 assignment of cloud motion vectors. A method has been developed to directly
353 correct motion vectors heights with nearby lidar cloud top observations, at first in
354 an experimental framework with airborne observations during a field campaign
355 (WEISSMANN et al., 2013) and subsequently using CALIPSO observations
356 (FOLGER and WEISSMANN, 2014). The developed lidar correction leads to a
357 significant reduction of motion vector wind errors by 12-17%. Further studies will
358 assess the benefit of such a correction for data assimilation, both by directly
359 assimilating height-corrected motion vectors and through the development of
360 situation-dependent correction functions.

361

362 **3.3 Model Development**

363 The overall aim of the HErZ Clouds and Convection (HErZ-CC) branch is to
364 better understand the physical processes that control the lifecycle of clouds and
365 convection and to use this understanding to improve their representations in
366 NWP models. Clouds are a decisive part of NWP and climate models. They
367 interconnect the land surface, planetary boundary layer and the deeper
368 atmosphere and allow for a range of complex scale interactions. As some of
369 these processes can be explicitly represented whereas other ones have to be
370 parameterized, the treatment of clouds, even in high-resolution weather
371 forecasts, essentially remains an unsolved problem. Most existing
372 parameterizations make either explicitly or implicitly assumptions about scale-
373 separation, convective quasi-equilibrium and sub-grid homogeneity which are
374 becoming a road block for further improvements of NWP and climate models.

375

376 **3.3.1 Large-eddy simulations (LESs)**

377 Improving parameterizations requires better understanding of the processes at
378 work as parameterizations encapsulate an idealization of our understanding.
379 Today supercomputers make it possible to perform LESs with grid spacings of
380 some 10-100 m on mesoscale domains over periods of several days. Such
381 simulations provide the data to develop and test new parameterization
382 hypotheses and they may also be used to estimate necessary parameters or
383 functions. Process studies with LESs constitute the first line of research in HErZ-

384 CC. It is here to emphasize that the best use of LESs is in improving our
385 understanding of the processes and their interactions, not in reproducing reality.

386 Figure 5 shows the result of such an LES of precipitating shallow cumulus
387 clouds on a domain of 50^2 km^2 with an isotropic grid spacing of 25 m. Such a
388 setup is able to resolve the larger turbulent eddies in the boundary layer, the
389 internal circulations of the clouds as well as the mesoscale flow which leads to
390 the self-organization of the cloud field (SEIFERT and HEUS, 2013). Figure 5
391 shows the simulated albedo of a cumulus field with the typical cloud patterns as
392 observed in the trade wind zones. These are the cloud streets that are due to
393 along-wind oriented boundary layer rolls, the so-called mesoscale arcs, regions
394 of deeper congestus-type clouds which may reach 4-6 km cloud top height and
395 can produce locally intense precipitation and cloud-free areas in between. The
396 LES data and additional sensitivity studies suggest that the main cause of the
397 organization are cold pools originating from the most intense rain events.
398 However, the cold pools are relatively weak and short lived, i.e. the mesoscale
399 patterns do not so much establish themselves in the temperature field, but only in
400 the moisture field itself. Hence, modelling the structure and statistics of the sub-
401 cloud layer moisture field as it evolves due to the effects of precipitation is key for
402 a parameterization which aims at representing the effect of cloud organization.

403 The cloud microphysics and radiation scheme of the LES model have also
404 been extended to allow the simulation of deep convection (HOHENEGGER and
405 STEVENS, 2013; SCHLEMMER and HOHENEGGER, 2014) and a simple land
406 surface model (RIECK et al., 2014) has been introduced. This enables the
407 investigation of the full diurnal cycle of convection, from shallow to deep,
408 including the interaction with the land surface.

409

410 **3.3.2 Understanding and parameterizing the cloud size distribution**

411 The cloud size distribution (CSD) constitutes the second line of research in
412 HErZ-CC. By providing explicit information about the size of all clouds, the goal is
413 to derive parameterizations that are appropriate for a given mesh size and are at
414 the same time able to provide information about sub-grid variability. It is worth
415 noting that the original proposal of the mass flux convection scheme by
416 ARAKAWA and SCHUBERT (1974) included the explicit prediction of different
417 cloud sizes, i.e. a cloud size distribution. This concept has later been largely
418 abandoned and replaced by the simpler bulk mass flux scheme (TIEDTKE, 1989;
419 PLANT, 2010). Including explicit assumptions about the size, life time and life
420 cycle of convective clouds may also be a necessary pre-requisite for a consistent
421 treatment of cloud microphysics and rain formation. For example, SEIFERT and
422 STEVENS (2010) suggested that the use of dynamical and microphysical
423 timescales may be a viable and promising alternative to the current formulation of
424 microphysical parameterizations within convection schemes.

425 Having large-eddy simulations for several cloud regimes makes it possible to
426 improve our understanding of small-scale variability and hence, to formulate
427 improved parameterizations. Based on such data, NAUMANN et al. (2013)
428 derived a refined cloud closure, which has now been handled over to DWD for
429 practical implementation and testing. Another major effort has been the

430 development of a cloud tracking algorithm which is able to handle extensive
431 datasets and at the same time includes a physically-based definition of cloud
432 objects (HEUS and SEIFERT, 2013). The clustering of clouds, which becomes
433 especially pronounced in the presence of precipitation, requires splitting clouds
434 into dynamically meaningful entities which is done based on the buoyant cloud
435 cores. Using cloud tracking, a power law size distribution for the instantaneous
436 shallow cumulus cloud field is found as it is also found based on satellite
437 observations. At the same time, LES data provide detailed information on the
438 cloud lifetime and cloud life-cycle which is necessary for the formulation of a
439 stochastic cloud scheme, e.g. following PLANT and CRAIG (2008).

440 Changes in the CSD as the clouds transition to deep convection or due to
441 heterogeneous surface conditions have also been investigated. In general, it is
442 thought that a widening of the clouds as the diurnal cycle proceeds constitutes
443 one of the necessary ingredients for transition to deep convection (e.g.
444 KHAIROUTDINOV and RANDALL 2006; KUANG and BRETHERTON 2006).
445 Understanding mechanisms that influence the size of the largest clouds is
446 therefore crucial. As soon as clouds begin to precipitate, the formation of cold
447 pools shifts the CSD to larger scales and promotes the transition to deep
448 convection (SCHLEMMER and HOHENEGGER, 2014). Figure 6 shows a
449 snapshot of a cloud field transitioning to deep convection. New clouds form on
450 the rim of the cold pools (visible as circular dry areas in Fig. 6), where moisture
451 has been accumulated. The size of the largest clouds seems to correlate with the
452 size of these moist patches. Likewise, surface heterogeneities can affect the
453 formation of larger clouds (RIECK et al., 2014). Except for such changes in the
454 scale break (i.e. largest clouds), the CSD remains remarkably similar over
455 homogeneous and heterogeneous surfaces. Accurately representing the effects
456 of cold pools and surface heterogeneity in convective parameterizations is thus
457 important to capture a correct timing of the development of convection. The
458 transition time from shallow to deep convection was for instance reduced by half
459 in a simulation performed over a heterogeneous surface with a heterogeneity
460 length scale of 12.8 km. Such effects are unlikely to be correctly represented,
461 even in cloud-resolving NWP models and may explain a delayed onset of
462 precipitation in such models.

463

464 **3.4 Climate Monitoring and Diagnostics**

465 The overall aim of HErZ-Climate is to develop and improve methods for the
466 self-consistent assessment and analysis of regional climate in Germany and
467 Europe over the past decades at an appropriate spatial and temporal resolution.
468 The central approach to this is the development and evaluation of a model-based,
469 high-resolution regional reanalysis system which encompasses the synergetic
470 use of heterogeneous monitoring networks while providing detailed diagnostics of
471 the energy, water and momentum cycles of the reanalysed climate state.

472 In the scope of climate monitoring, reanalyses are becoming more and more
473 important for the assessment of climate variability and climate change. The
474 European Union Global Monitoring for Environment and Security (GMES)
475 initiative has recently started funding for generating reanalyses and the

476 verification of the corresponding data sets. These efforts are directed towards
477 establishing climate services based on reanalyses. HErZ-Climate takes part in
478 the EU-FP7 funded projects UERRA (Uncertainties in Ensembles of Regional
479 Reanalysis) as well as CORE-CLIMAX in order to provide impetus for the
480 continuous development, production and dissemination of regional reanalyses
481 towards a climate services framework.

482

483 **3.4.2 Criteria for regional reanalyses**

484 Within the meteorological and climate community, the term reanalysis is
485 commonly understood as the synthesis of past observations – heterogeneous in
486 space and time – into a physical model using a state-of-the-art assimilation
487 system. By freezing the model and data assimilation system, it avoids systematic
488 variations that otherwise appear in operational NWP analyses. Such a model-
489 based approach yields the advantage of generating 4D fields for a large number
490 of atmospheric variables, which are physically consistent in space and time as
491 well as between the parameters.

492 Gridded climate data products based on alternative approaches such as
493 spatio-temporal interpolation methods do not meet these criteria. Commonly
494 used atmospheric reanalyses include ERA-Interim (ECMWF Re-Analysis, DEE et
495 al., 2011) and MERRA (Modern-Era Retrospective analysis for Research and
496 Applications, RIENECKER et al., 2011) by the National Oceanic and
497 Atmospheric Administration (NOAA). Such reanalyses facilitate a large
498 observational data set, a global circulation model and a corresponding data
499 assimilation scheme. The horizontal grid-spacing of global reanalyses is usually
500 in the range of 70-125 km and the temporal resolution of the output normally
501 coincides with the 6-h interval between two assimilation cycles, sometimes
502 complemented by the output of 3-h forecasts. For a better representation of
503 spatio-temporal variability including local extreme events, the regional
504 enhancement of global reanalysis data has become an important task. An
505 approach for the European region is presented in sections 3.4.3 and 3.4.4.

506 The added value of high-resolution regional reanalyses lies in the enhanced
507 representation of spatio-temporal variability and extremes and, most importantly,
508 in the spatio-temporal coherence with independent observations. SIMON et al.
509 (2013) showed that regional dynamical downscaling methods generate variability
510 in the inner-domain by itself, whereas data assimilation on regional scales
511 suppresses this freely developing variability.

512 Such regional reanalysis systems provide a quality-controlled and
513 homogenised data set for the detection and assessment of regional climate
514 change in the past and the future, the statistical post-processing of operational
515 forecasts, the analysis of systematic model errors of the respective regional
516 model as well as the verification and calibration of climate impact models.

517

518 **3.4.3 Regional reanalysis for the European CORDEX domain**

519 HErZ-Climate generated a high-resolution regional reanalysis for the CORDEX
520 EUR-11 domain (COordinated Regional Downscaling Experiment, cf. Fig. 7), but
521 with an increased resolution of the horizontal grid to 0.055° (~6 km). The

522 reanalysis consists of the DWD COSMO model and its nudging (or dynamical
523 relaxation) assimilation system. The atmospheric analysis is complemented by a
524 soil moisture, a sea surface temperature and a snow analysis module. In a first
525 stream, reanalysis data have been produced for the period 2007-2011. The
526 following part of this section provides findings from the comparison of COSMO-
527 REA6 and ERA-Interim. A detailed analysis including various parameters can be
528 found in BOLLMEYER et al. (2014).

529 At first, precipitation estimates of the two reanalyses against rain gauge
530 observations over Germany have been evaluated. The difficulty when evaluating
531 the quality of precipitation estimates is that it follows a non-Gaussian distribution
532 and therefore standard scores such as bias or RMSE are inadequate. Therefore,
533 histograms of 3-hourly precipitation over Germany were analysed in order to
534 investigate the quality of precipitation reanalyses.

535 Histograms for the observations, COMSO-REA6 and ERA-Interim are
536 presented in Figure 8. The diagrams show the frequency of occurrence for weak
537 (upper panel) and heavy precipitation events (lower panel). For the frequent
538 weak precipitation events, COSMO-REA6 performs well compared to
539 observations while ERA-Interim shows an underestimation of event frequency for
540 values below 0.1 mm and above 5 mm per 3 h. For values of 0.1-5 mm per 3 h,
541 ERA-Interim overestimates the frequencies of events.

542 For the less frequent heavy precipitation events, the histogram bins are
543 restricted to values above 20 mm per 3 h. COSMO-REA6 underestimates the
544 frequencies of the observed precipitation, especially in the range of 20-30 mm.
545 However, COSMO-REA6 still represents extreme precipitation events, with the
546 frequency of occurrence being well-estimated for precipitation events of 50 mm
547 and beyond. In contrast, ERA-Interim does not exhibit values that exceed 22 mm
548 in 3 h at all. This is in accordance with the change of support as rain gauge
549 observations are point measurements while reanalyses represent area-averaged
550 values.

551 The results from the first stream of COSMO-REA6 underline the added value
552 of high-resolution regional reanalyses as a tool to monitor regional climate. The
553 increased resolution allows a better representation of surface parameters and
554 meso-scale processes leading to an improved reproduction of local variability of
555 the climate such as extreme events. Especially in the context of severe weather,
556 the understanding of climate variability on these scales is becoming more and
557 more important.

558

559 **3.4.4 Towards a regional reanalysis on the convection-permitting scale**

560 Currently, the production of a horizontally refined convection-permitting scale
561 reanalysis is under way. With 2-km grid size for a domain covering Germany and
562 adjacent areas (Fig. 7), the reanalysis COSMO-REA2 allows the direct
563 representation of deep convection. The reanalysis is supported by a latent heat
564 nudging (LHN) scheme which assimilates radar data to allow for a better
565 representation of rainfall.

566 First results of COSMO-REA2 for summer 2011 indicate that the precipitation
567 analysis is further improved, especially with regard to the diurnal cycle. Figure 9

568 shows the precipitation intensity for all 3-h intervals of the day for June, July and
569 August 2011. In comparison to the observed precipitation, it can be observed that
570 ERA-Interim does not represent the diurnal cycle with precipitation intensities
571 remaining nearly constant throughout the day. In COSMO-REA6, a diurnal cycle
572 is present with the correct amplitude but lagged by approximately 3 h while in
573 COSMO-REA2 the diurnal cycle is reproduced nearly perfectly, thereby showing
574 the benefits of a convection-permitting reanalysis.

575

576 **3.5 Communication and Use of Forecasts and Warnings**

577 At the end of the forecasting process, the value of forecasts is only
578 accomplished if end users make better decisions, e.g. to mitigate the impact of
579 hazardous weather. In order to be able to make optimal use of the information
580 contained in the forecast, the users' vulnerability must be known and suitable
581 mitigation measures must be available. Furthermore, forecasting products must
582 be disseminated reliably, they must be understood and accepted. All these
583 aspects of optimal forecast usage can only be investigated by a transdisciplinary
584 approach including social sciences, relevant institutions and stakeholders.

585 Research on this final step of the forecasting process has been scarce in
586 Germany, yet there have been some efforts in the United States and Australia
587 (e.g. the "Weather And Society - Integrated Studies" (WAS-IS) initiative) or in the
588 United Kingdom (ROULSTON et al., 2006) and the topic has been addressed in
589 the World Weather Research Programme (WWRP) and the THORPEX
590 programme of the World Meteorological Organization (WMO, 2004).

591 HERZ-Application investigates weather warnings and their perception and use
592 by emergency managers and the public. The applied methods range from
593 statistical modelling to surveys, direct observations of emergency managers and
594 stakeholder interviews. The main focus in the initial phase of HERZ are warnings
595 for wind storms and thunderstorms in Berlin. The goal is to improve the warning
596 process and the communication of warnings and to develop recommendations
597 for user-oriented information products. One overarching aspect is the treatment
598 of uncertainty information.

599

600 **3.5.1 Estimation and perception of uncertainty**

601 Although weather warnings are uncertain, they are still delivered without an
602 explicit indication of their weather-dependent uncertainty. To investigate the
603 usefulness of uncertainty information for emergency managers, a test product
604 has been designed with the help of DWD's regional office responsible for Berlin.
605 It consists of probabilistic short range forecasts of warning events for 6-h time
606 intervals. As a first step, this human-made forecast has been verified and
607 compared to a statistical forecast. Both forecasts were very reliable, at least for
608 moderately severe events. Note, that this good calibration of the forecasters has
609 been achieved without providing feedback to them yet.

610 DWD provides weather warning information to emergency managers via the
611 online platform FeWIS (Feuerwehr-Wetterinformationssystem). Access to this
612 platform is limited to emergency managers from dispatch centres, professional,
613 voluntary and private fire brigades and other relief units. An online survey on this

614 platform has been conducted to assess how much emergency managers are
615 aware of uncertainties, how much trust they put in the information and how they
616 are affected by failed weather warnings. In a previous survey, FRICK and HEGG
617 (2011) investigated the users' assessment of and trust in a similar Swiss online
618 platform for hydrologic and atmospheric hazards. 174 FeWIS users responded:
619 59% represent fire brigades and dispatch centres, 26% are emergency
620 managers and 14% belong to other relief units. The survey showed that 60% of
621 respondents rated the frequency of false alarms at least as "acceptable". Only
622 13% of participants replied that false alarms are too frequent or much too
623 frequent.

624 Another question was how participants estimated the frequency of false
625 alarms. The vast majority of emergency managers expects thunderstorms to
626 occur for 60-90% of warnings (Fig. 10). The objectively verified rate of
627 occurrence of an event after a thunderstorm warning was issued by DWD
628 however, is significantly lower. Depending on the regional forecast centre, the
629 rate is in the range of 40-55% (GÖBER, 2012). It is unclear whether
630 meteorologists and emergency managers define false alarms in the same way. A
631 thunderstorm for example, that hits uninhabited regions or does not cause
632 missions might not be perceived as an event by EMs. Thus, emergency
633 managers put high trust into weather warnings issued by DWD although they are
634 aware of uncertainties.

635 An open question was posed about the consequences of false alarms. 35% of
636 responders claimed to suffer no consequences. About two thirds prepared for an
637 event, mostly by reinforcing staff for relief missions and dispatch centres by
638 prolonging work shifts, setting up standby duty or calling in voluntary fire
639 brigades. One quarter of survey participants reported that they took
640 precautionary measures, which then turned out to be not needed. Those
641 measures included cancelling outdoor events, checking equipment and installing
642 defences. Roughly 20% of emergency managers raised the concern that false
643 alarms cause reduced trust in warnings by both DWD and their own institution.

644 Complementary to the effects of false alarms, the consequences of missed
645 events have been investigated. Here, only 10% of respondents claimed to suffer
646 no consequences. 35% of respondents were troubled by lacking of staff in
647 dispatch centres and for rescue forces. The former is particularly critical if it leads
648 to a queuing of emergency calls. The latter means to alert and wait for
649 reinforcements and therefore causes a delay of counter measures and
650 emergency responses. Additionally, reinforcing personnel might be obstructed by
651 weather effects.

652 Another 35% of respondents suffered from being unprepared. Resources and
653 material were not available and emergency managers struggled to keep track of
654 the situation and to plan missions. Probably the most severe consequence is
655 putting people at risk (when not sending out warnings, e.g. to outdoor events)
656 and suffering avoidable damage. This was named in 20% of the answers. Loss of
657 trust was listed only by 3% of responders.

658 Another online survey aimed at a larger audience within the emergency
659 management community: KOX et al. (2014) investigated the perception and use

660 of uncertainty information in severe weather warnings. The results showed that
661 the emergency service personnel who participated in this survey generally had a
662 good appraisal of uncertainty in weather forecasts. When asking for a probability
663 threshold at which mitigation actions would start, a broad range of values was
664 mentioned and a tendency to avoid decisions based on low probabilities was
665 detected. Furthermore, additional uncertainty was noted to arise from linguistic
666 origins, e.g. context dependence, underspecificity, ambiguity and vagueness.

667

668 **3.5.2 Risk analysis and risk communication**

669 The vulnerability of people and infrastructure plays a major part in the analysis
670 of risks, especially for large cities. One important aspect of risk mapping is the
671 distribution of trees, since storm damaged trees pose a major threat, e.g. to
672 people, cars or rail tracks. Here, Berlin is particularly vulnerable since its 5342
673 km of streets are lined, on average, by about 80 trees per km. Trees are stressed
674 in cities because of water deficiency, heat, pollution, bad soil conditions, small
675 rooting spaces, etc. Inter alia, this leads to a weakening of wood or defence
676 against insect attacks. Vulnerability is dependent on tree species and age (wood
677 flexibility), size (height, crown), foliage and other factors.

678 Mass media are the major public source of information about impending
679 severe weather (ULBRICH, 2013). A content analysis of television weather
680 reports of the 26 most severe winter storms has been conducted with the goal to
681 relate the information and its quality to observed and modelled losses (DONAT et
682 al., 2011). In a semi-experimental setting, the understanding of TV weather
683 reports has been tested with about 200 students in order to investigate how they
684 perceived and understood the information and whether they derived actions from
685 it.

686

687 **4 Summary and outlook**

688 The initial phase of HErZ has triggered a number of activities in the areas of
689 weather forecasting and climate research. Basic research within HErZ
690 complements more applied internal research at DWD. In addition, HErZ
691 significantly intensifies the collaboration between universities, research
692 institutions and DWD. This is seen as a benefit for both the host institutions and
693 DWD. Training young scientist is also a key component of HErZ. All branches are
694 actively involved in course teaching and several special training events have
695 been conducted. In addition, a number of doctoral, master and bachelor students
696 have completed or are working on their thesis in the framework of HErZ.

697 HErZ has been established as a virtual research centre and contributes to
698 better understanding of atmospheric processes, ways to observe and represent
699 them in numerical models and ways to forecast them to mitigate their impact.
700 Specific contributions of the current HErZ to improved understanding address:

- 701 • The structure, life-cycle, precipitation efficiency and organization of shallow
702 and deep convection;
- 703 • The differences between convective-scale and synoptic-scale data
704 assimilation;

- 705 • Representation of different sources of uncertainty in ensemble systems;
- 706 • The effects of land surface heterogeneities and soil moisture on the formation
- 707 of convective clouds;
- 708 • Regional and local climate variability;
- 709 • The perception and use of forecasts.

710 In addition to an improved understanding, a number of specific methods, tools
711 and data sets have been developed in HErZ. In the course of future phases of
712 HErZ, the research shall feed into improved modelling, monitoring and
713 forecasting capabilities. More specifically, research of HErZ shall lead to:

- 714 • Seamless short-term weather prediction by means of a more detailed
- 715 process description in nowcasting and high-resolution data assimilation;
- 716 • Improved assimilation systems through additional observations and new
- 717 tools;
- 718 • Improved and scale-adaptive parameterizations of clouds and convection;
- 719 • Improved monitoring of past weather and climate;
- 720 • Improved communication and use of forecast uncertainty and weather
- 721 warnings.

722 The five branches of HErZ address different aspects of weather or climate
723 research, but they share common research topics as for example regional high-
724 resolution (km-scale) modelling. Clouds, convection and hydrometeors are
725 another important aspect for the first four branches and research ranges from
726 polarimetric radar observations to cloud tracking, cloud motion vectors,
727 assimilation of cloud observations, idealized LES of cloud regimes, suitable
728 parameterizations and cloud validation. Further joint research areas include
729 observation forward operators, data assimilation, probabilistic forecasting and the
730 verification and validation of analyses and forecasts.

731 The current HErZ research covers the whole chain of topics relevant for
732 weather forecasting and climate monitoring ranging from understanding of
733 processes over methods to represent these in observation-based nowcasting
734 and numerical models to ways of condensing and communicating the
735 observational and model-based information to end users. By this, it brings
736 together basic with applied research, observational with modelling expertise,
737 academic with weather service experience and scientists with end users.

738 HErZ has overcome the difficulty of initiating and establishing such an
739 unprecedented collaboration of DWD, universities and research institutes. It has
740 triggered and intensified research in important, as yet underrepresented subjects
741 at universities. The remaining challenges for the long-term success of HErZ will
742 be to develop sustainable structures based on currently limited-term funding for
743 the branches and long-term career perspectives for people working in HErZ.
744 Establishing the centre has also been accompanied by comparably high
745 management efforts given the centre's strategic and structural goals in addition
746 to research objectives. Thus, finding a good balance between structural demands
747 and the focus on its primary objective of excellent science as well as a good
748 balance of fundamental research and research motivated by and focused on
749 needs of a weather service are seen as crucial tasks for lasting scientific

750 success.

751

752 **Acknowledgement**

753 The presented research was carried out in the Hans-Ertel Centre for Weather
754 Research. This German research network of universities, research institutes and
755 DWD is funded by the BMVBS (Federal Ministry of Transport, Building and Urban
756 Development). Furthermore, the authors want to acknowledge the Scientific
757 Advisory Committee of DWD and particularly Mr. Wolfgang Kusch, Prof. Clemens
758 Simmer and Prof. Gerhard Adrian for their efforts to initiate this unique
759 collaboration of universities, research institutes and DWD.

760

761 **References**

- 762 ARAKAWA, A., W.H. SCHUBERT, 1974: Interaction of a Cumulus Cloud
763 Ensemble with the Large-Scale Environment, Part I. – J. Atmos. Sci. 31, 674–
764 701.
- 765 BENGTSSON, L., 2001: The development of medium range forecasts. In: *50th*
766 *Anniversary of Numerical Weather Prediction, Commemorative Symposium*
767 *Potsdam 9-10 March 2000, Germany*. Ed. A. Spekat, 119-138.
- 768 BETZ, H.D., K. SCHMIDT, P. LAROCHE, P. BLANCHET, W. OETTINGER, E.
769 DEFER, Z. DZIEWIT, J. KONARSKI, 2009: LINET - An international lightning
770 detection network in Europe. – Atmos. Res. 91, 564–573.
- 771 BJERKNES, V., 1904: Das Problem der Wettervorhersage, betrachtet vom
772 Standpunkt der Mechanik und Physik. – Meteorol. Z. 21, 1–7.
- 773 BLEY, S.H. DENEKE, 2013: A robust threshold-based cloud mask for the HRV
774 channel of MSG SEVIRI. – Atmos. Meas. Tech. 6, 2713–2723.
- 775 BOLLMEYER, C., J.D. KELLER, C. OHLWEIN, S. BENTZIEN, S. CREWELL, P.
776 FRIEDERICHS, K. HARTUNG, A. HENSE, J. KEUNE, S. KNEIFEL, I.
777 PSCHIEDT, S. REDL, S. STEINKE, 2014: Towards a high-resolution regional
778 reanalysis for the European CORDEX domain. – Quart. J. Roy. Meteor. Soc.,
779 submitted.
- 780 CRAIG, G.C., M. WÜRSCH, 2013: The impact of localization and observation
781 averaging for convective-scale data assimilation in a simple stochastic model.
782 – Quart. J. Roy. Meteor. Soc. 139, 515–523.
- 783 COMANICIU, D., P. MEER, 2002: Mean Shift: A Robust Approach Toward
784 Feature Space Analysis. – IEEE Transactions on Pattern Analysis and
785 Machine Intelligence 24, 603–619.
- 786 DEE, D.P., S.M. UPPALA, A.J. SIMMONS, P. BERRISFORD, P. POLI, S.
787 KOBAYASHI, U. ANDRAE, M.A. BALMASEDA, G. BALSAMO, P. BAUER, P.
788 BECHTOLD, A.C.M. BELJAARS, L. VAN DE BERG, J. BIDLOT, N.
789 BORMANN, C. DELSOL, R. DRAGANI, M. FUENTES, A.J. GEER, L.
790 HAIMBERGER, S.B. HEALY, H. HERSBACH, E.V. HÓLM, L. ISAKSEN, P.
791 KÅLLBERG, M. KÖHLER, M. MATRICARDI, A.P. MCNALLY, B.M. MONGE-
792 SANZ, J.-J. MORCRETTE, B.-K. PARK, C. PEUBEY, P. DE ROSNAY, C.
793 TAVOLATO, J.-N. THÉPAUT, F. VITART, 2011: The ERA-Interim reanalysis:
794 configuration and performance of the data assimilation system. – Quart. J. Roy.
795 Meteor. Soc. 137, 553–597.

796 DENEKE, H., R. ROEBELING, 2010: Downscaling of METEOSAT SEVIRI 0.6
797 and 0.8 micron channel radiances utilizing the high-resolution visible channel.
798 – Atmospheric Chemistry and Physics 10, 9761–9772.

799 DIETZSCH, F., 2013: Validierung satellitenbasierter Früherkennung konvektiver
800 Gewitter mittels Rückwärtstrajektorien, Master's thesis, Faculty of Physics and
801 Earth Sciences, University of Leipzig.

802 DONAT, M.G., T. PARDOWITZ, G.C. LECKEBUSCH, U. ULBRICH, O.
803 BURGHOFF, 2011: High-Resolution refinement of a storm loss model and
804 estimation of return periods of loss-intensive storms over Germany. – Natural
805 Hazards and Earth System Sciences 11, 2821–2833.

806 EDWARDS, P.N., 2010: A vast machine: computer models, climate data, and the
807 politics of global warming. MIT press, Cambridge, ISBN 978-0-262-01392-5.

808 FOLGER, K., M. WEISSMANN, 2014: Height correction of atmospheric motion
809 vectors using satellite lidar observations from CALIPSO. – J. Appl. Meteor.
810 Climatol., DOI: <http://dx.doi.org/10.1175/JAMC-D-13-0337.1>.

811 FRICK, J., C. HEGG, 2011: Can end-users' flood management decision making
812 be improved by information about forecast uncertainty? – Atmos. Res., 100,
813 296–303.

814 GÖBER, M., 2012: Verifikationsbericht zur Güte lokaler Wetterprognosen. No. 45.
815 Deutscher Wetterdienst.

816 GRAMELSBERGER, G., 2009: Conceiving meteorology as the exact science of
817 the atmosphere: Vilhelm Bjerknes's paper of 1904 as a milestone. – Meteorol.
818 Z. 18, 669-673.

819 HENSE, A., V. WULFMEYER, 2008: The German Priority Program SPP1167
820 “Quantitative Precipitation Forecast”. – Meteorol. Z. 17, 703-705.

821 HEUS, T., A. SEIFERT, 2013: Automated tracking of shallow cumulus clouds in
822 large domain, long duration large eddy simulations. – Geosci. Model Dev. 6,
823 1261–1273.

824 HOHENEGGER, C., B. STEVENS, 2013: Preconditioning deep convection with
825 cumulus congestus. – J. Atmos. Sci. 70, 448–464.

826 HORVÁTH, Á., K. WAPLER, F. SENF, H. DENEKE, M. DIEDRICH, J. SIMON, S.
827 TRÖMEL, 2012: Lagrangian analysis of precipitation cells using satellite, radar,
828 and lightning observations. Ext. Abstracts, 2012 EUMETSAT Meteorological
829 Satellite Conference, 3-7 September 2012, Sopot, Poland.

830 HUNT, B.R., E.J. KOSTELICH, I.S. ZUNYOGH, 2007: Efficient data assimilation
831 for spatiotemporal chaos: A local ensemble transform kalman filter. – Physica
832 D 230, 112–126.

833 IPCC, 2012: Managing the Risks of Extreme Events and Disasters to Advance
834 Climate Change Adaptation. A Special Report of Working Groups I and II of
835 the Intergovernmental Panel on Climate Change [Field, C.B., V. Barros, T.F.
836 Stocker, D. Qin, D.J. Dokken, K.L. Ebi, M.D. Mastrandrea, K.J. Mach, G.-K.
837 Plattner, S.K. Allen, M. Tignor, P.M. Midgley (eds.)]. Cambridge University
838 Press, Cambridge, UK, and New York, USA, 582 pp.

839 JAKOB, C., 2010: Accelerating progress in global atmospheric model
840 development through improved parametrizations - Challenges, opportunities
841 and strategies. – Bull. Amer. Meteorol. Soc. 91, 869–875.

842 JANJIC, T., D. MCLAUGHLIN, S.E. COHN, M. VERLAAN, 2014: Conservation of
843 mass and preservation of positivity with ensemble-type Kalman filter
844 algorithms. – *Mon. Weather Rev.* 142, 755–773.

845 KALNAY, E., Y. OTA, T. MIYOSHI, J. LIU, 2012: A simpler formulation of
846 forecast sensitivity to observations: application to ensemble Kalman filters. –
847 *Tellus A* 64, 18462.

848 KEIL, C., F. HEINLEIN, G.C. CRAIG, 2014: The convective adjustment time-
849 scale as indicator of predictability of convective precipitation. – *Quart. J. Roy.*
850 *Meteor. Soc.*, DOI:10.1002/qj.2143.

851 KHAIROUTDINOV, M., D. RANDALL, 2006: High-resolution simulation of
852 shallow-to-deep convection transition over land. – *J. Atmos. Sci.* 63, 3421–
853 3436.

854 KOSTKA, P.M., M. WEISSMANN, R. BURAS, B. MAYER, O. STILLER, 2014:
855 Observation Operator for Visible and Near-Infrared Satellite Reflectances. – *J.*
856 *Atmos. Ocean. Technol.*, DOI: <http://dx.doi.org/10.1175/JTECH-D-13-00116.1>.

857 KOX, T., L. GERHOLD, U. ULBRICH, 2014: Perception and use of uncertainty in
858 severe weather warnings by emergency services in Germany. – *Atmos. Res.*,
859 DOI: <http://dx.doi.org/10.1016/j.atmosres.2014.02.024>

860 KUANG, Z., C.S. BRETHERTON, 2006: A mass-flux scheme view of a high-
861 resolution simulation of a transition from shallow to deep cumulus convection.
862 – *J. Atmos. Sci.* 63, 1895–1909.

863 KÜHNLEIN, C., C. KEIL, G.C. CRAIG, C. GEBHARDT, 2014: The impact of
864 downscaled initial condition perturbations on convective-scale ensemble
865 forecasts of precipitation. – *Quart. J. Roy. Meteor. Soc.*, DOI: 10.1002/qj.2238,

866 LANGE, H., G.C. CRAIG, 2014: On the benefits of a high resolution analysis for
867 convective data assimilation of radar data using a local ensemble Kalman filter.
868 – *Mon. Weather Rev.*, submitted.

869 LORENZ, E.N., 1995: Predictability: A problem partly solved. – In *Proc. Sem.*
870 *Predictability* 1, 1–18.

871 MILAN, M., D. SCHUETTEMAYER, T. BICK, C. SIMMER, 2014: A Sequential
872 Ensemble Prediction System at Convection-Permitting Scales. – *Meteorology*
873 *and Atmospheric Physics* 123, 17-31.

874 NAUMANN, A.K., A. SEIFERT, J.P. MELLADO, 2013: A refined statistical cloud
875 closure using double-Gaussian probability density functions. – *Geosci. Model*
876 *Dev.* 6, 1641–1657.

877 PLANT, R.S., 2010: A review of the theoretical basis for bulk mass flux
878 convective parameterization. – *Atmos. Chem. Phys.* 10, 3529-3544.

879 PLANT, R.S., G.C. CRAIG, 2008: A Stochastic Parameterization for Deep
880 Convection Based on Equilibrium Statistics. – *J. Atmos. Sci.* 65, 87–105.

881 REICH, H., A. RHODIN, C. SCHRAFF, 2011: LETKF for the nonhydrostatic
882 regional model COSMO-DE. *COSMO Newsletter* 11, 27–31. Available at
883 [http://www.cosmo-](http://www.cosmo-model.org/content/model/documentation/newsLetters/newsLetter11)
884 [model.org/content/model/documentation/newsLetters/newsLetter11](http://www.cosmo-model.org/content/model/documentation/newsLetters/newsLetter11).

885 REMPEL, M., 2013: Gewittervorhersage auf dem Prüfstand - Möglichkeiten der
886 objekt-basierten COSMO-DE Validierung mittels Satellitenprodukt RDT.
887 Bachelor's thesis, Faculty of Physics and Earth Sciences, University of Leipzig.

888 RIECK, M., C. van HEERWAARDEN, C. HOHENEGGER, 2014: The influence of
889 land surface heterogeneity on cloud size development. – *Mon. Weather Rev.*,
890 submitted.

891 RIENECKER, M.M., M.J. SUAREZ, R. GELARO, R. TODLING, J. BACMEISTER,
892 E. LIU, M.G. BOSILOVICH, S.D. SCHUBERT, L. TAKACS, G.-K. KIM, S.
893 BLOOM, J. CHEN, D. COLLINS, A. CONATY, A. DA SILVA, G. WU, J.
894 JOINER, R.D. KOSTER, R. LUCCHESI, A. MOLOD, T. OWENS, S. PAWSON,
895 P. PEGION, C.R. REDDER, R. REICHLE, F.R. ROBERTSON, A.G. RUDDICK,
896 M. SIENKIEWICZ, J. WOOLLEN, 2011: MERRA – NASA's Modern-Era
897 Retrospective Analysis for Research and Applications. – *J. Climate* 24, 3624–
898 3648.

899 ROSENFELD, D., D. ATLAS, D.A. SHORT, 1990: The Estimation of Convective
900 Rainfall by Area Integrals, 2. The Height-Area Rainfall Threshold (HART)
901 Method. – *J. Geophys. Res.* 95, 2161–2176.

902 ROULSTON, M.S., G.E. BOLTON, E.N. KLEIT, A.L. SEARS-COLLINS, 2006: A
903 laboratory study of the benefits of including uncertainty information in weather
904 forecasts. – *Weather Forecasting* 21, 116–122.

905 RYZHKOV, A., M. DIEDRICH, C. SIMMER, 2013: Potential utilization of specific
906 attenuation for rainfall estimation, mitigation of partial beam blockage, and
907 radar networking. – *J. Atmos. Ocean. Technol.*, 31, 599–619.

908 SCHLEMMER, L., C. HOHENEGGER, 2014: The formation of wider and deeper
909 clouds as a result of cold-pool dynamics. – *J. Atmos. Sci.*, DOI:
910 <http://dx.doi.org/10.1175/JAS-D-13-0170.1>.

911 SEIFERT, A., T. HEUS, 2013: Large-eddy simulation of organized precipitating
912 trade wind cumulus clouds. – *Atmos. Chem. Phys.* 13, 5631–5645.

913 SEIFERT, A., B. STEVENS, 2010: Microphysical Scaling Relations in a
914 Kinematic Model of Isolated Shallow Cumulus Clouds. – *J. Atmos. Sci.* 67,
915 1575–1590.

916 SENF, F., H. DENEKE, M. DIEDRICH, Á. HORVÁTH, C. SEIMMER, J.L. SIMON,
917 S. TRÖMEL, K. WAPLER, 2012: On severe convective storms over Central
918 Europe: satellite products within a case study. *Proceedings of 2012*
919 *EUMETSAT Meteorological Satellite Conference*, 3-7 September 2012, Sopot,
920 Poland.

921 SIEWERT, C.W., M. KOENIG, J.R. MECIKALSKI, 2010: Application of Meteosat
922 second generation data towards improving the nowcasting of convective
923 initiation. – *Met. Apps* 17, 442–451.

924 SIMON, T., D. WANG, A. HENSE, C. SIMMER, C. OHLWEIN, 2013: Generation
925 and transfer of internal variability in a regional climate model. – *Tellus A* 65,
926 22485.

927 SOMMER, M., M. WEISSMANN, 2014: Observation Impact in a Convective-
928 Scale Localized Ensemble Transform Kalman Filter. – *Quart. J. Roy. Meteor.*
929 *Soc.*, DOI: 10.1002/qj.2343.

930 TIEDTKE, M., 1989: A Comprehensive Mass Flux Scheme for Cumulus
931 Parameterization in Large-Scale Models. – *Mon. Weather Rev.* 117, 1779–
932 1800.

933 TRÖMEL, S., C. SIMMER, J. BRAUN, T. GERSTNER, M. GRIEBEL, 2009:
934 Towards the use of Integral Radar Volume Descriptors for quantitative areal
935 precipitation estimation - results from pseudo-radar observations. – J. Atmos.
936 Ocean. Technol. 26, 1798–1813.

937 TRÖMEL, S., C. SIMMER, 2012: An object-based approach for areal rainfall
938 estimation and validation of atmospheric models. – Meteorol. Atmos. Phys.,
939 115, 139–151.

940 TRÖMEL, S., M. KUMJIAN, A. RYZHKOV, C. SIMMER, M. DIEDRICH, 2013a:
941 Backscatter differential phase - estimation and variability. – J. Appl. Meteor.
942 Climatol. 52, 2529–2548.

943 TRÖMEL, S., A.V. RYZHKOV, M.R. KUMJIAN, P. ZHANG, C. SIMMER, 2013b:
944 The measurements of backscatter differential phase δ in the melting layer at X
945 and S bands. Proceedings of AMS Radar Conference, 16-20 September 2013,
946 Breckenridge, Colorado, U.S.
947 <https://ams.confex.com/ams/36Radar/webprogram/Paper228548.html>

948 ULBRICH, H., 2013: Medien und Bevölkerung. Rezeption von Sturmwarnungen
949 in TV-Wetterberichten. – Crisis Prevention 3/2013, 14–15.

950 VAN LEEUWEN, P.J., 2009: Particle filtering in geophysical systems. – Mon.
951 Weather Rev. 137, 4089–4114.

952 VAN LEEUWEN, P.J., 2011: Efficient non-linear data assimilation in geophysical
953 fluid dynamics. – Computers and Fluids, DOI:10.1016/j.compfluid.2010.11.011.

954 VOLKERT, H., D. ACHERMANN, 2012: Roots, foundation, and achievements of
955 the “Institut für Physik der Atmosphäre”. In: Atmospheric Physics: background
956 – methods - trends. "Research Topics in Aerospace", Springer-Verlag Berlin,
957 843-860, ISBN 978-3-642-30182-7.

958 WAPLER, K., M. GÖBER, S. TREPTE, 2012: Comparative verification of
959 different nowcasting systems to support optimisation of thunderstorm warnings.
960 – Adv. Sci. Res. 8, 121–127.

961 WAPLER, K., 2013: High-resolution climatology of lightning characteristics within
962 central Europe. – Meteorol. Atmos. Phys. 122, 175-184.

963 WAPLER, K., P. JAMES, 2014: Thunderstorm occurrence and characteristics in
964 Central Europe under different synoptical conditions. – Atmos. Res., submitted.

965 WEISSMANN, M., R.H. LANGLAND, P.M. PAULEY, S. RAHM, C. CARDINALI,
966 2012: Influence of airborne Doppler wind lidar profiles on ECMWF and
967 NOGAPS forecasts. – Quart. J. Roy. Meteor. Soc. 138, 118–130.

968 WEISSMANN, M., K. FOLGER, H. LANGE, 2013: Height correction of
969 atmospheric motion vectors using airborne lidar observations. – J. Appl.
970 Meteor. Climatol. 52, 1868–1877.

971 WMO, 2004: THORPEX. A Global Atmospheric Research Programme.
972 International Science Plan. WMO/TD-No. 1246, WWRP/THORPEX No. 2.

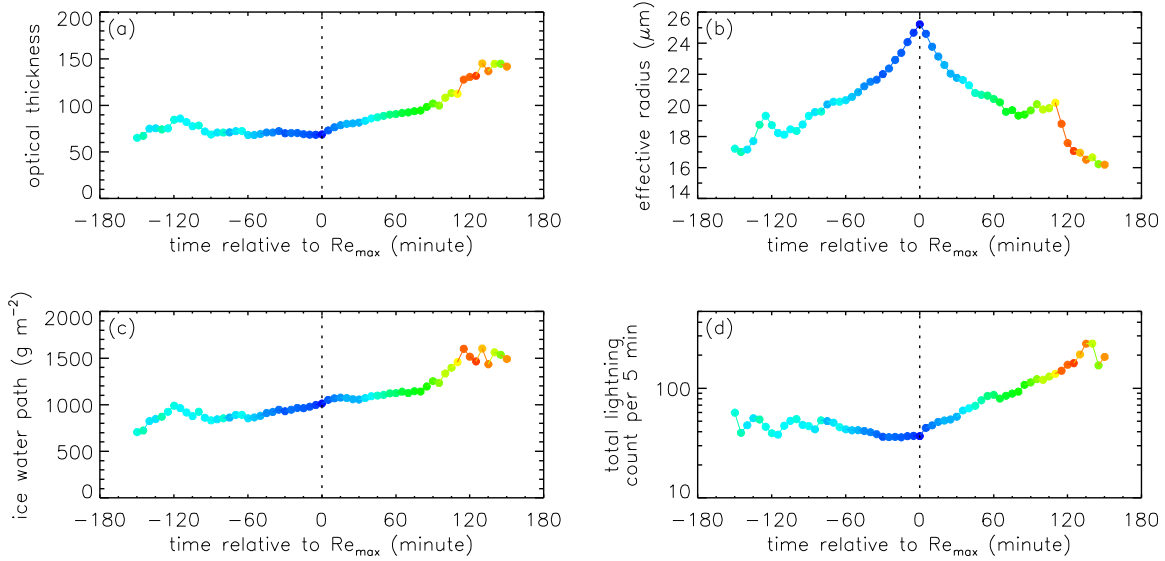
973 WULFMEYER, V., A. BEHREND, H.-S. BAUER, C. KOTTMEIER, U.
974 CORSMEIER, A. BLYTH, G. CRAIG, U. SCHUMANN, M. HAGEN, S.
975 CREWELL, P. DI GIROLAMO, C. FLAMANT, M. MILLER, A. MONTANI, S.
976 MOBBS, E. RICHARD, M.W. ROTACH, M. ARPAGAU, H.
977 RUSSCHENBERG, P. SCHLÜSSEL, M. KÖNIG, V. GÄRTNER, R.
978 STEINACKER, M. DORNINGER, D.D. TURNER, T. WECKWERTH, A.

979 HENSE, C. SIMMER, 2008: The Convective and Orographically-induced
980 Precipitation Study: A Research and Development Project of the World
981 Weather Research Program for improving quantitative precipitation forecasting
982 in low-mountain regions. – Bull. Amer. Meteor. Soc. 89, 1477-1486.
983 WÜRSCH, M., G.C. CRAIG, 2014: A simple dynamical model of cumulus
984 convection for data assimilation research. – Meteorol. Z., DOI: 10.1127/0941-
985 2948/2014/0492.
986 ZRNIĆ, D.S., A.V. RYZHKOV, J. STRAKA, Y. LIU, J. VIVEKANANDAN, 2001:
987 Testing a Procedure for automatic classification of hydrometeor types. – J.
988 Atmos. Ocean. Technol. 18, 892–913.

Branch topic and affiliated authors	Project title, research topics and host institutions	Branch short name
Atmospheric dynamics and predictability; <i>S. Trömel,</i> <i>K. Wapler,</i> <i>H. Deneke</i>	Object-based Analysis and SEamless prediction (OASE); <ul style="list-style-type: none"> • Synergistic use of multi-sensor observations • Analysis of the structure and life-cycle of deep convection • Nowcasting and (very) short-term forecasting of severe weather events <i>Universität Bonn, Leibniz-Institut für Troposphärenforschung Leipzig</i>	Branch 1: HErZ-OASE
Data Assimilation; <i>M. Weissmann,</i> <i>T. Janjic</i>	Ensemble-based convective-scale data assimilation and the use of remote sensing observations <ul style="list-style-type: none"> • Methods and tools for convective-scale data assimilation • Use of cloud-related satellite observations • Representing uncertainty in ensemble systems <i>Ludwig-Maximilians-Universität München</i>	Branch 2: Data Assimilation (HErZ-DA)
Model development; <i>C. Hohenegger,</i> <i>A. Seifert</i>	Clouds and convection <ul style="list-style-type: none"> • Process studies with large-eddy simulations • Analysis and characterization of the cloud size distribution • Improved parameterizations of subgrid processes <i>Max-Planck Institut für Meteorologie, Hamburg</i>	Branch 3: Clouds and Convection (HErZ-CC)
Climate monitoring and diagnostics; <i>C. Ohlwein,</i> <i>J. Keller,</i> <i>C. Bollmeyer</i>	Retrospective analysis of regional climate; <ul style="list-style-type: none"> • Development of a regional reanalysis system • Assimilation techniques for historical observation systems • Diagnostics of the energy, water, and momentum cycles <i>Universität Bonn, Universität zu Köln</i>	Branch 4: HErZ-Climate
Communication and use of forecasts and warnings; <i>T. Ulbrich,</i> <i>M. Göber</i>	Improving the process of weather warnings and extreme weather information in the chain from the meteorological forecasts to their communication for the Berlin conurbation (WEXICOM) <ul style="list-style-type: none"> • Assessment of uncertainty of weather warnings • Analysis of risk communication and perception • Analysis of vulnerability and risk management <i>Freie Universität Berlin, Forschungsforum Öffentliche Sicherheit, Deutsches Komitee Katastrophenvorsorge</i>	Branch 5: HErZ-Application

990 Table 1: The five branches of HErZ in the initial funding phase 2011-2014.

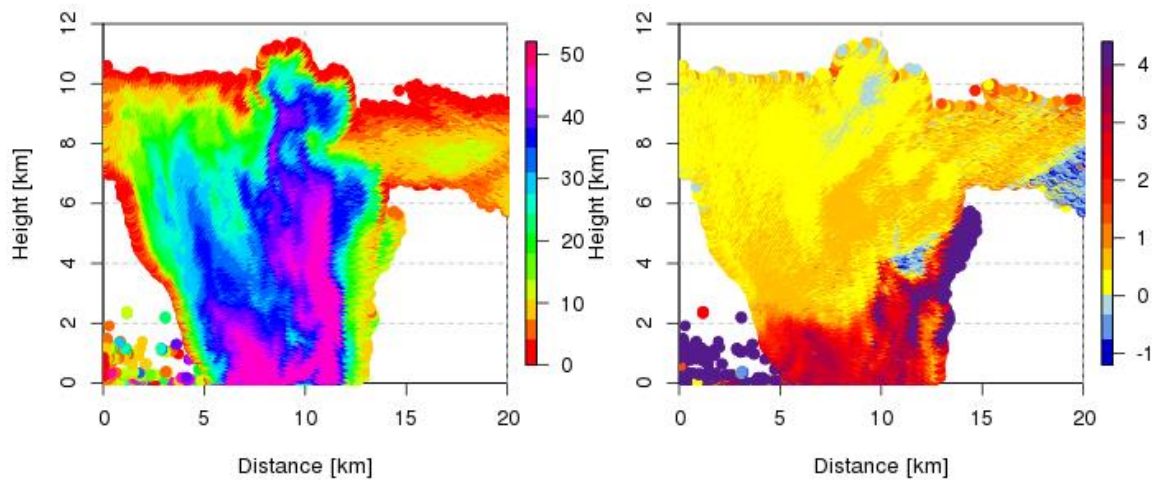
991 Figures



992

993

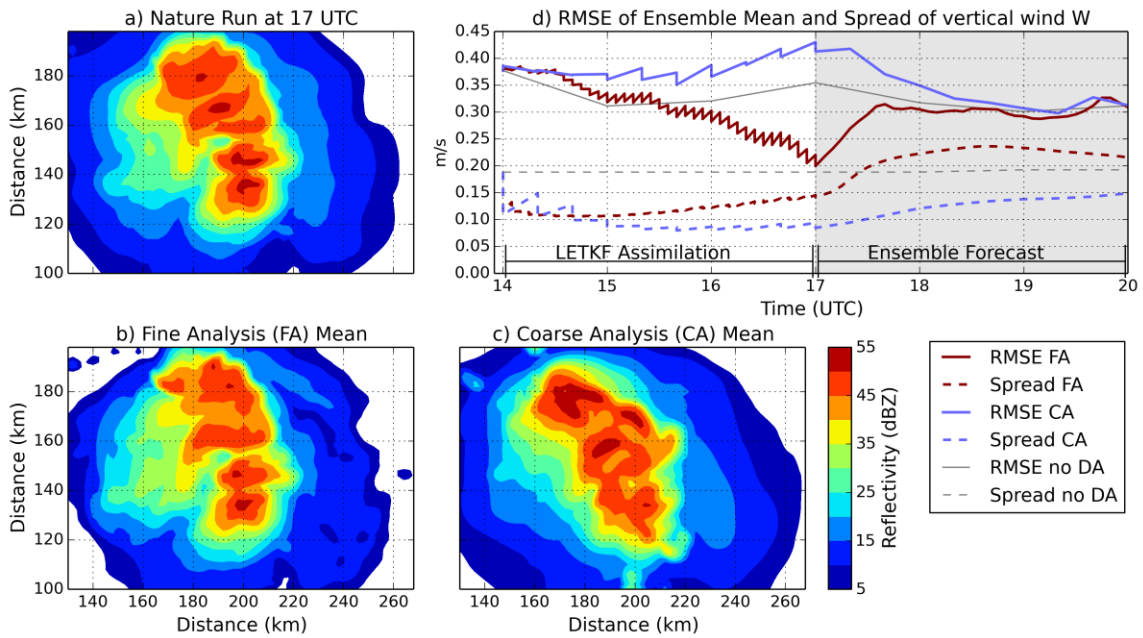
994 Figure 1: Evolution of satellite-retrieved cloud properties and ground-based total
995 lightning count per 5 min time interval averaged over ~1700 systems tracked with
996 KONRAD and synchronized to the time of maximum effective radius (vertical
997 dotted line). The colour indicates the KONRAD cell size, i.e. number of radar
998 pixels (1 km^2) with reflectivity greater 46 dBZ, ranging from less than or equal to
999 30 (blue) to greater than or equal to 120 (red).



1000

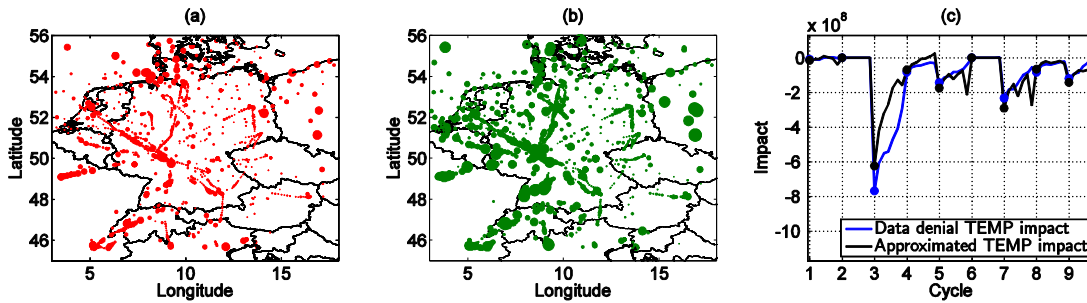
1001

1002 Figure 2: Vertical cross-section of a storm during intense lightning activity from
 1003 measurements of the polarimetric X band radar in Bonn (BoxPo) on 5 June 2011
 1004 at 1359 UTC. The left panel shows the horizontal reflectivity Z_H (in dBZ) and the
 1005 right panel the differential reflectivity Z_{DR} (in dB).



1006

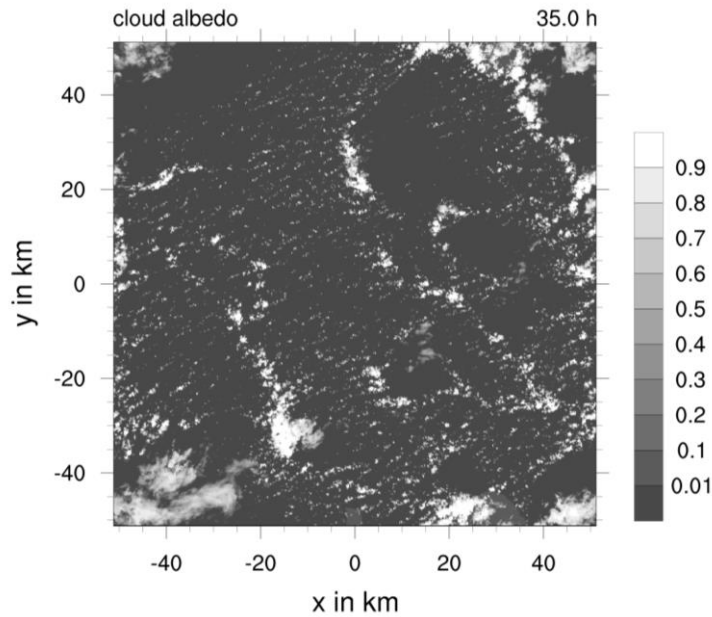
1007 Figure 3: Idealized experiments to investigate convective-scale radar assimilation
 1008 with an ensemble Kalman filter. (a) Composite radar reflectivity of the nature
 1009 (“truth”) run, (b) the corresponding ensemble mean of the fine analysis (FA) and
 1010 (c) of the coarse analysis scheme (CA) after 3 h of cycled data assimilation.
 1011 (d) RMSE and spread of vertical velocity of FA (red) CA (blue) and the
 1012 experiment without data assimilation (no DA, grey) during cycled assimilation
 1013 (white area) and free forecast (grey area).



1014

1015

1016 Figure 4: Spatial distribution of approximated impact for all observations with
 1017 beneficial (a) and detrimental (b) impact with marker size proportional to the
 1018 impact values. Forecast time 6 h from initialization at 8 August 2009 1200 UTC.
 1019 (c) Data denial (blue) and approximated (black) impact of radiosonde
 1020 observations. Dots represent the analysis influence and lines the evolution of the
 1021 observation impact for forecast lead times up to 6 h from every analysis cycle.



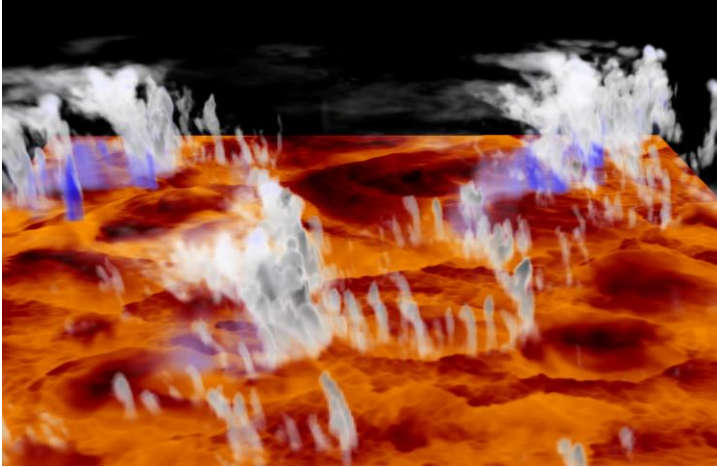
1022

1023

1024 Figure 5: Synthetic cloud albedo for the RICO LES case as calculated from
 1025 simulated cloud liquid water path after 35 h. Shown is the result of a simulation
 1026 with the UCLA-LES model using $4096 \times 4096 \times 160$ grid points with an isotropic
 1027 mesh of 25 m grid spacing. The resulting domain has a horizontal size of $100 \times$
 1028 100 km and can therefore include mesoscale cloud structures as the mesoscale
 1029 arcs that are typically observed in precipitating shallow convection in the trade
 1030 wind zone.

1031

1032

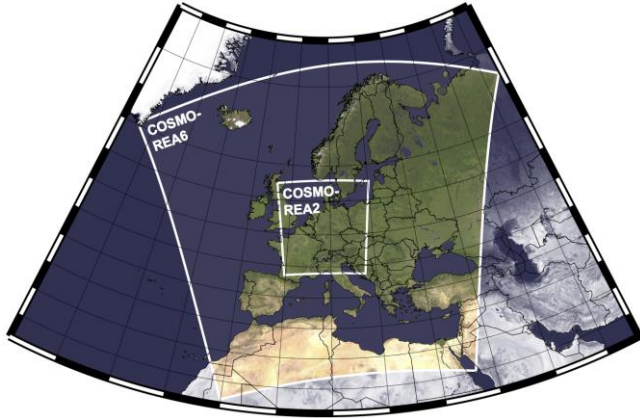


1033

1034

1035 Figure 6: 3D snapshot of developing deep convection with cloud (white),
1036 precipitation (blue) and near-surface humidity (from low to high: black-red-orange)
1037 from a LES simulation (grid spacing 100 m, domain size 125 x 125 km).

1038

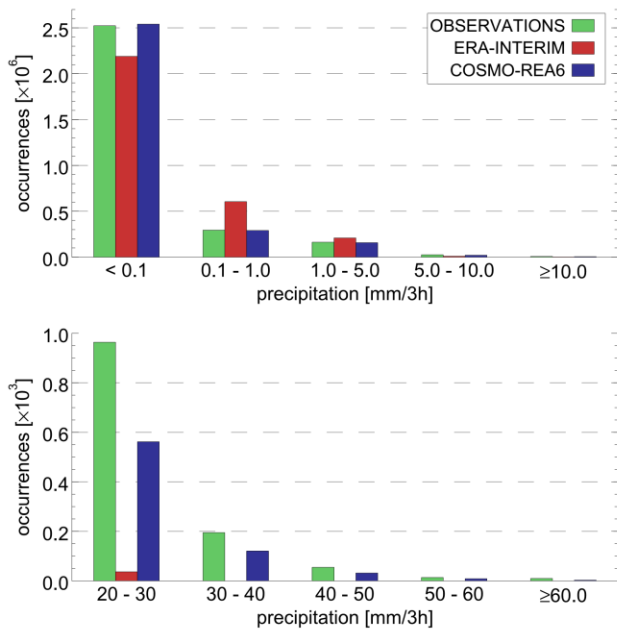


1039

1040

1041 Figure 7: A map of Europe showing the domains for the European reanalysis
1042 (COSMO-REA6, approx. 6 km resolution, 880x856 grid points) and the
1043 German reanalysis (COSMO-REA2, approx. 2 km resolution, 724x780 grid
1044 points).

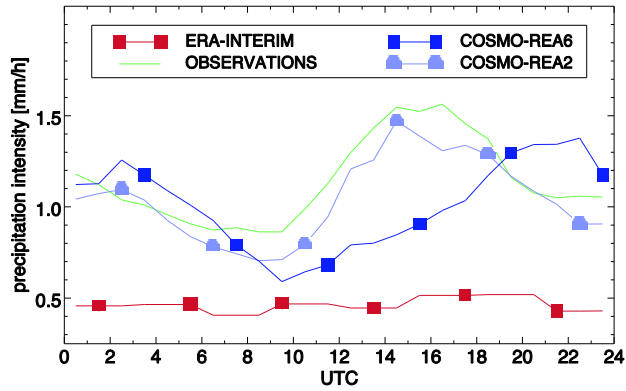
1045



1046

1047 Figure 8: Histograms of 3-hourly precipitation over Germany for 2011 for rain
 1048 gauge observations (green), ERA-Interim (red) and COSMO-REA6 (blue) for
 1049 weak (upper diagram) and heavy (lower diagram) precipitation events.

1050



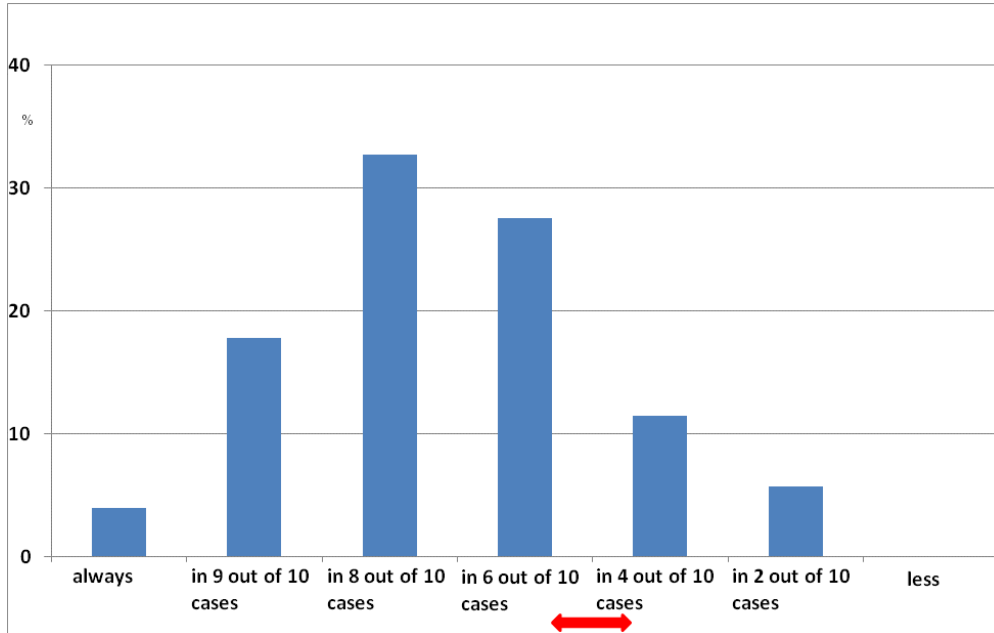
1051

1052

1053 Figure 9: Diurnal cycle of precipitation intensity (3-hourly averages) for June
 1054 2011 over Germany. Values for the observations (green), ERA-Interim (red),
 1055 COSMO-REA6 (dark blue) and COSMO-REA2 are shown.

1056

1057



1058

1059

1060 Figure 10: Participants of the online survey were asked: "When receiving a
1061 thunderstorm warning via FeWIS, how often do you expect a thunderstorm to
1062 actually happen?" The red arrow indicates the range of the objectively verified
1063 rate of occurrence of an event in a county after a thunderstorm warning was
1064 issued (GÖBER, 2012).

1065

1066